



# Combination of cyclic voltammetry and single-particle Brownian dynamics methodology to evaluate the fluidity of phospholipid monolayers at polarized liquid/liquid interfaces

Andrea V. Juárez<sup>a, c, e</sup>, Ana V. Juárez<sup>a, c, e, \*</sup>, Natalia Wilke<sup>b, d, e</sup>, Lidia M. Yudi<sup>a, c, e, \*\*</sup>

<sup>a</sup> Universidad Nacional de Córdoba, Facultad de Ciencias Químicas, Departamento de Físicoquímica, Córdoba, Argentina

<sup>b</sup> Universidad Nacional de Córdoba, Facultad de Ciencias Químicas, Departamento de Química Biológica "Ranwel Caputto", Córdoba, Argentina

<sup>c</sup> Consejo Nacional de Investigaciones Científicas y Técnicas, CONICET, Instituto de Investigaciones en Físicoquímica de Córdoba, INFIQC, Córdoba, Argentina

<sup>d</sup> Consejo Nacional de Investigaciones Científicas y Técnicas, CONICET, Centro de Investigaciones en Química Biológica de Córdoba, CIQUIBIC, Córdoba, Argentina

<sup>e</sup> Haya de la Torre y Medina Allende, Ciudad Universitaria, X5000HUA, Argentina

## ARTICLE INFO

### Article history:

Received 26 March 2018

Received in revised form

13 May 2018

Accepted 17 May 2018

Available online 30 May 2018

### Keywords:

Liquid/liquid interfaces

Phospholipids monolayers

Monolayers fluidity

Latex microbeads

Single-particle Brownian dynamics

## ABSTRACT

The present work shows, for the first time, the use of single-particle Brownian dynamics methodology, followed by optical microscopy, coupled with electrochemistry techniques to evaluate the fluidity of phospholipid films adsorbed at liquid/liquid interfaces. The combination of the two methods allows observing the movement of latex beads at the liquid/liquid interface modified by a phospholipid monolayer, with and without polarization by linear potential scans or potential steps. In this way, the effect of polarization on distearoylphosphatidylglycerol (DSPG), dimyristoylphosphatidylcholine (DMPC), and distearoylphosphatidylcholine (DSPC) monolayers, adsorbed at the water/1,2-dichloroethane interface, could be directly observed and diffusion coefficient values were derived. Lateral motilities of these particles can be correlated with the monolayer fluidity and solid character. A comparison with the behavior of the lipids at air/water interfaces is also included.

© 2018 Elsevier Ltd. All rights reserved.

## 1. Introduction

The interface between two immiscible electrolyte solutions (ITIES) modified by a phospholipid monolayer has been widely studied in order to understand their structure and permeability. Following this purpose, different methodologies have been employed, among which cyclic voltammetry [1–8] impedance [9,10] and surface tension techniques using a Langmuir trough [11–16] can be mentioned. Also, the interaction with other biomolecules [17–19] and polyelectrolyte's [20,21] was studied. The electrochemical study of monolayers generated by the Langmuir [12] or Langmuir–Blodgett [13–16] methods represents an important progress in the knowledge and control of the state of

these films. All references listed above demonstrate that electrochemical techniques applied at the ITIES are ideal to follow dynamic changes in the lipid layer compactness and interfacial interactions at a hydrophobic/hydrophilic boundary [21].

When a phospholipids solution is injected at a liquid/liquid interface the molecules spontaneously orientate their polar head groups inside the aqueous side of the interface and the hydrocarbon chains into the organic phase, perpendicular to the interfacial plane. The polar head group modifies the electrical properties of the interface [22] and produces important interactions with different cations present in the aqueous phase [2,23–25]. It's important to study the dependence of the film stability with the interfacial potential difference and the changes in the coverage during the experiment. In that sense, the present work shows, for the first time, the changes carried out by a phospholipid monolayer adsorbed at a liquid/liquid interface, when a potential difference is applied, employing single particle tracking methods, which allows comparing the fluidity of the film before and after the potential perturbation.

Several works reported the study of the diffusion properties of

\* Corresponding author. Universidad Nacional de Córdoba, Facultad de Ciencias Químicas, Departamento de Físicoquímica, Córdoba, Argentina.

\*\* Corresponding author. Universidad Nacional de Córdoba, Facultad de Ciencias Químicas, Departamento de Físicoquímica, Córdoba, Argentina.

E-mail addresses: [vjuarez@fcq.unc.edu.ar](mailto:vjuarez@fcq.unc.edu.ar) (A.V. Juárez), [mjudi@fcq.unc.edu.ar](mailto:mjudi@fcq.unc.edu.ar) (L.M. Yudi).

membranes following the Brownian motion of latex microbeads or lipids domains [26–34] at the air/liquid interface. Lateral motilities of these particles embedded into the monolayer can be correlated with the film viscosities through the usual hydrodynamic relationships and, in this way, infer about the solid character or the fluidity of the monolayers. In the present paper, the motion of the microbeads at a liquid/liquid interface formed by water/1,2-dichloroethane solutions was followed by optical microscopy and their diffusion coefficients,  $D$ , were determined before and after polarization.

## 2. Experimental

### 2.1. Materials

The phospholipids employed, 1,2-dimyristoyl-*sn*-glycero-3-phosphocholine (DMPC), 1,2-distearoyl-*sn*-glycero-3-phosphocholine (DSPC), 1,2-distearoyl-*sn*-glycero-3-phospho-(1'-*rac*-glycerol) (sodium salt) (DSPG) and the lipophilic fluorescent probe L- $\alpha$ -phosphatidylethanolamine-N-(lissaminerhodamine B sulfanyl) (ammonium salt) (egg-transphosphatidylated, chicken) (Rho-egg PE) were purchased from Avanti Polar Lipids (Alabaster, AL). Fig. 1 shows the chemical structure of phospholipids employed.

Lipid solutions were prepared in  $\text{Cl}_3\text{CH}/\text{CH}_3\text{OH}$  2:1 v/v, with all the solvents and chemicals used being of the highest commercial purity available. The aqueous solutions were prepared with deionized water (with resistivity of 18  $\text{M}\Omega$ , obtained from a Milli-Q Gradient System, Millipore, Bedford, MA).

Micrometer-sized beads (0.9  $\mu\text{m}$  mean diameter, carboxylate-modified latex beads, CLB9) were purchased from SIGMA. The beads were cleaned by successive centrifugation and re-suspension of the pellet in clean Milli-Q water. This procedure was repeated 10 times and then they were re-suspended in water, forming a concentrated clean bead solution ( $10^{10}$  beads/mL).

For the electrochemical experiments  $\text{CaCl}_2$  (Sigma Aldrich, p.a. grade) was used as the salt for the aqueous supporting electrolyte, while the organic phase contained tetrapentylammonium tetrakis (4-chlorophenyl) borate (TPnATCIPB) dissolved in 1,2-dichloroethane (1,2-DCE, Dorwill). TPnATCIPB was synthesized by metathesis of tetrapentylammonium bromide (TPnABr, Sigma Aldrich) and potassium tetrakis (4-chlorophenyl) borate (KTCIPB, Sigma Aldrich).

### 2.2. Surface pressure measurements

Phospholipids monolayers at liquid/liquid (L/L) and at air/water (A/L) interfaces were generated in a glass cell of 3.94  $\text{cm}^2$  geometrical area, containing the subphase (for experiments at A/L interfaces) or both phases (for experiments at L/L interfaces), in the last case with the organic one at the bottom. L/L interfaces were formed between an aqueous phase containing 10 mM  $\text{CaCl}_2$ , pH = 5, and an organic phase containing TPnATCIPB 10 mM in 1,2-dichloroethane, while a subphase containing 10 mM  $\text{CaCl}_2$ , pH 5.0 was used for the studies at A/L interfaces.

The surface tension was measured by the Wilhelmy plate method with a platinum plate, using a KSV Instruments Ltd. (Helsinki, Finland). The Wilhelmy plate was placed at the A/L or at the L/L interface with 25% of its geometrical area immersed into the organic phase (L/L experiments) or the subphase (A/L experiments). In the case of measurements at L/L interfaces special care has been taken that both faces of the Wilhelmy plate were wet with the organic solution, with a concave meniscus. Under these conditions, the surface pressure for the L/L interface in the absence of the monolayer was between 24 and 26  $\text{mN m}^{-1}$ . This pressure value was set as zero and then successive volumes of 0.50 mg/mL DSPG, DMPC, or DSPC solutions were carefully spread at the surface, with a Hamilton microsyringe (Reno, NV, USA), recording the surface pressure after 1 min of stabilization, when a constant pressure value was reached. The isotherm was plotted from this data set.

All measurements were performed at 25  $^\circ\text{C}$ . The determined mean molecular areas were highly reproducible, with a typical area and collapse pressure errors of  $\pm 2 \text{ \AA}^2$  and  $\pm 1 \text{ mN m}^{-1}$ , respectively. They were obtained from at least three isotherms for each condition.

### 2.3. Fluorescence and phase contrast microscopy

Fluorescence microscopy (FM) was carried out at A/L and L/L interfaces, employing Rho-egg PE as fluorescent. This fluorescent amphiphile was incorporated in the phospholipid solution, at a molar ratio Rho-egg: phospholipid 1:99, before spreading the monolayer. The probe was employed with the purpose of observing and focusing the L/L interface. Once the interface was focused, phase contrast microscopy was employed to observe the microbeads present at the interface. The experiments involving A/L

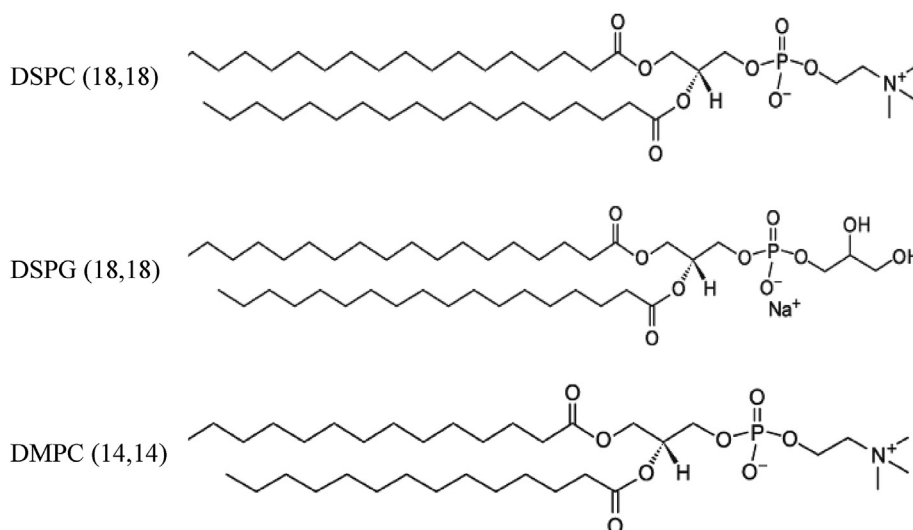


Fig. 1. Chemical structure of phospholipids employed.

interfaces were performed in a Langmuir film balance (micro-through, Kibron, Helsinki, Finland), which was placed on the stage of an inverted fluorescence microscope (Axiovert 200, Carl Zeiss, Oberkochen, Germany) with an LD 20× objective (air immersion). Images were registered by a CCD video camera (IxonEM + model DU-897, Andor Technology). Instead, for the experiments concerning to L/L interfaces, a direct fluorescence microscope (Axio-plan, Carl Zeiss, Oberkochen, Germany) with 63× objective (water immersion) and a CCD video camera Axio CamHRc (Carl Zeiss, Oberkochen, Germany) were used.

For the analysis of the latex bead motion, images with phase contrast microscopy were recorded. The aqueous subphase, in the case of the studies carried out at A/L interfaces, or the organic phase, for the studies at L/L interfaces, were reduced to a thickness of about 3 mm to minimize convection. For the observation of the L/L interface the objective is immersed in the aqueous phase and placed very close to the interface. Only 2D movements of the latex beads were registered.

#### 2.4. Diffusion coefficient of microbead in lipid monolayers

A small amount of the bead suspension was carefully spread at the liquid/liquid interface in the presence or the absence of the monolayer with a Hamilton microsyringe. The final bead density was normally about 1 bead in 2000–2500  $\mu\text{m}^2$ . This low amount of beads did not affect the mean molecular area nor the collapse pressure and the general surface behavior of lipid monolayers.

The diffusion coefficient of micrometer-sized beads was calculated as previously described [27] at surface pressure of 9  $\text{mNm}^{-1}$  for L/L interface and 20  $\text{mNm}^{-1}$  for A/L interface. In the L/L system, when polarization experiments were carried on, the diffusion coefficients of beads were measured 30s after the polarization. Briefly, movies of the monolayer surface at the liquid/liquid or air/liquid interface were recorded (200 frames, 14 frames/s). Then, the relative positions of micro beads selected in pairs were followed through the 200 frames. The mean square displacement of a bead relative to another ( $\text{MSD}_{\text{rel}}$ ) was calculated for different time lapses between frames ( $\delta t$ ) as:

$$\text{MSD}_{\text{rel}} = \left( \left| \overline{X}_{\text{rel}}^{t+\delta t} - \overline{X}_{\text{rel}}^t \right|^2 \right) \quad (1)$$

$\text{MSD}_{\text{rel}}$  was plotted as a function of  $\delta t$  for each experimental condition. If the beads in the selected pair are in the same environment, the drift on each particle should be similar. In these

conditions,  $\text{MSD}_{\text{rel}} = 8D\delta t$  [29].

#### 2.5. Cyclic voltammetry and potential steps

Cyclic voltammetry (CV) and potential steps were carried out employing an electrochemical analyzer CHI C700. Electrochemical experiments were performed in a four-electrode system using the glass cell described before. Two platinum wires and two Ag/AgCl were immersed, at each phase, and employed as counter and reference electrodes respectively. The reference electrode in contact with the organic solution was immersed in an aqueous solution containing 10.0 mM tetrapentylammonium bromide (TPnABr, Sigma-Aldrich) and 10.0 mM  $\text{CaCl}_2$ .

The supporting electrolyte solutions were 10.0 mM  $\text{CaCl}_2$  in ultra-pure water and 10.0 mM TPnATCIPB in 1,2-dichloroethane. The pH of the aqueous solution was 5.0. The electrochemical cell used was as follows:

Ag	AgCl	TPnABr + $\text{CaCl}_2$ 10 mM (w')	TPnATCIPB 10 mM (o)	$\text{CaCl}_2$ 10 mM (w)	AgCl	Ag
----	------	---	---------------------------	---------------------------------	------	----

When CV is applied to a L/L system, the increase in current observed at extreme positive and negative potentials, is due to the transfer of the supporting electrolyte present in the aqueous or in the organic phase. In the middle of the potential window, only a reorganization of ions occurs in each phase, without interfacial ion transfer, depicting a capacitor behavior in this zone. In the case of potential steps, two different potential values were selected,  $E = 0.200$  and 0.950 V where faradaic current is observed, and  $E = 0.450$  V where only capacity processes are occurring, with the purpose to evaluated the lipids movements under different conditions.

The interfacial pressure was recorded while cyclic voltammetry was carried on at different scan rates: 5, 10, 50 and 100  $\text{mVs}^{-1}$ , or different potential steps: 0.200, 0.450 or 0.950 V, during 1min, were applied. For this purpose the measurement of interfacial pressure was carried out as described in section 2.2.

Fig. 2 shows a schematic view of the cell employed in the measurements on L/L interfaces, 2A: Simultaneous electrochemical techniques and surface pressure determination and 2B: coupled

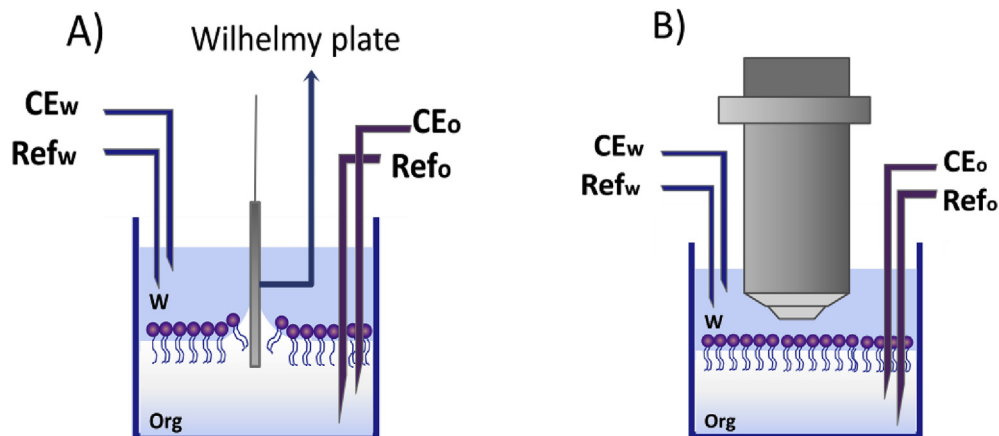


**Fig. 2.** Schematic view of the cell employed for experiments at L/L interfaces. A) Electrochemical system coupled with Langmuir balance. w: aqueous phase, org: organic phase.  $\text{CE}_w$  and  $\text{CE}_o$  are the Pt counter electrodes in each phase,  $\text{Ref}_w$  and  $\text{Ref}_o$  are the reference electrode Ag/AgCl in the aqueous and the organic phase, respectively. B) Electrochemical system coupled with the microscope.

Microscopy and electrochemical techniques.

### 3. Results and discussion

Fig. 3 shows the isotherms corresponding to DSPC, DSPG and DMPC monolayers at both interfaces: L/L and A/L (inset). As it can be observed, the typical response for this kind of molecules was obtained at the A/L interface: the isotherm corresponding to DMPC reveals a more expanded monolayer, while the corresponding to DSPC and DSPG indicate the presence of more compact films, as it is expected from the hydrophobic chain lengths. The isotherms obtained at L/L interfaces show a similar tendency, but with a general decrease in collapse pressures and increase in molecular areas, compared to the values obtained at A/L interfaces. The decrease in the collapse pressure is expected since the surface tension on the bare L/L interface ( $\sim 25 \text{ mN m}^{-1}$ ) is about 3-times lower than that at the A/L interface ( $\sim 73 \text{ mN m}^{-1}$ ). The values of the collapse area evaluated from these isotherms are:  $110 \text{ \AA}^2/\text{molecule}$  for DMPC,  $59 \text{ \AA}^2/\text{molecule}$  for DSPC and  $51 \text{ \AA}^2/\text{molecule}$  for DSPG, which are significantly higher than those corresponding to air/water interfaces ( $53 \text{ \AA}^2/\text{molecule}$  for DMPC,  $40 \text{ \AA}^2/\text{molecule}$  for DSPC and  $39 \text{ \AA}^2/\text{molecule}$  for DSPG), probably due to the penetration of organic solvent molecules or organic ions within the hydrophobic tails [35,36]. This increment in the mean molecular areas led to a decrease in the film stiffness, i.e. the films at the liquid/liquid interface are more compressible. The compressibility coefficient obtained at  $9 \text{ mNm}^{-1}$  was  $39 \text{ mNm}^{-1}$  for DSPG,  $18 \text{ mNm}^{-1}$  for DSPC and  $9 \text{ mNm}^{-1}$  for DMPC, which are significantly lower than the values corresponding to A/L interfaces,  $341 \text{ mNm}^{-1}$  for DSPG,  $240 \text{ mNm}^{-1}$  for DSPC and  $90 \text{ mNm}^{-1}$  for DMPC.

These films were observed by microscopy. As an example, Fig. 4 shows the images obtained for DSPG, similar ones were observed for the other phospholipids studied. Fig. 4A shows a representative fluorescence image of a DSPG monolayer at the L/L interface, at  $\pi = 9 \text{ mNm}^{-1}$  employing Rho-egg PE as the probe. As can be observed, the film formed is heterogeneous, the dark regions (probe-deficient) are larger at high pressures. This heterogeneity might be related with a mixed lipid-organic solvent film, which is probably also the reason for the less solid feature of these films compared to that formed at the air-water interface. It is important to remark at this point, that the probe does not mix with this kind of very stiff films at the A/L interface, instead it remains segregated in very fluorescent spots [37]. Therefore, this is another difference

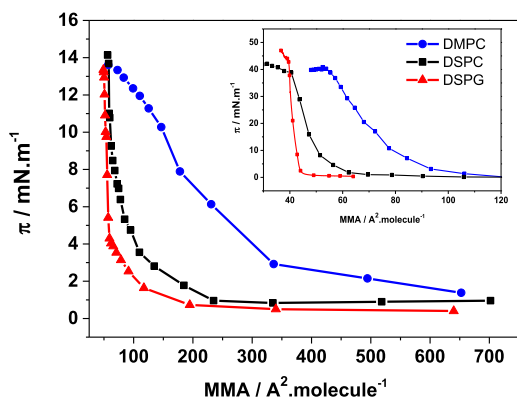


Fig. 3. Surface pressure ( $\pi$ ) vs mean molecular area isotherms for DMPC, DSPC and DSPG at the water/1,2-dichloroethane interface obtained as described in section 2.2 (Aqueous phase composition: 10 mM  $\text{CaCl}_2$ , Organic phase composition: TPnATCIPhB 10 mM in 1,2-dichloroethane). Inset: Surface pressure ( $\pi$ ) vs mean molecular area isotherms at the air/water interface obtained as described in section 2.2 (subphase composition: 10 mM  $\text{CaCl}_2$ ).

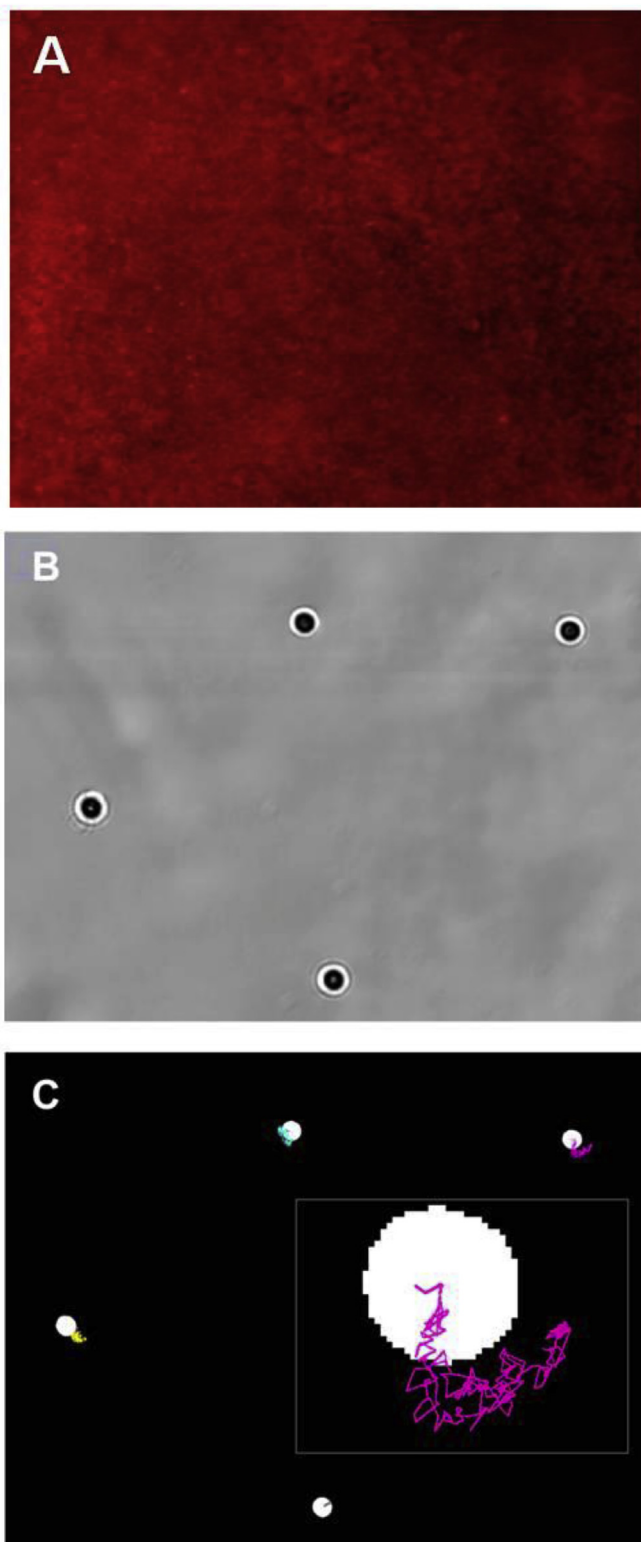
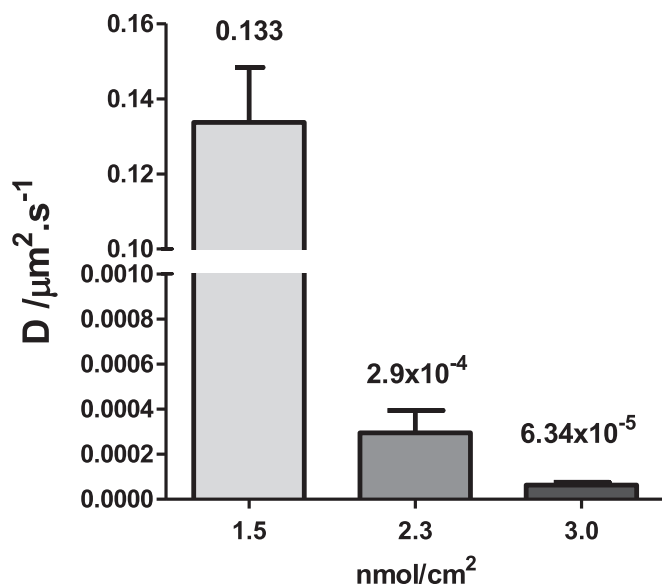


Fig. 4. A) Representative fluorescence image of a DSPG monolayer at the L/L interface, obtained at  $\pi = 9 \text{ mNm}^{-1}$ . Probe: Rho-egg PE. B) Representative image of latex microbeads obtained by contrast microscopy, at the DSPG monolayer adsorbed at the L/L interface ( $\pi = 9 \text{ mNm}^{-1}$ ). Aqueous phase composition: 10 mM  $\text{CaCl}_2$  in milliQ water. Organic phase composition: 10 mM TPnATCIPhB in 1,2-DCE. C) Binary Image of the same micrograph showing the Brownian displacement from which the diffusion coefficients were calculated. Scale Bar:  $5 \mu\text{m}$ .



**Fig. 5.** Diffusion coefficients of microlatex beads at DSPG monolayers adsorbed at L/L interface, employing different concentration of DSPG, expressed as nmol/cm<sup>2</sup> injected at the interface. Data are represented as mean  $D \pm SD$  of 40 individual pair of trajectories analyzed. Aqueous phase composition: CaCl<sub>2</sub> 10 mM in milliQ water; Organic phase composition: TPnATCIPhB 10 mM in 1,2-DCE.

between the films formed by DSPG at each interface and points to a less packed monolayer at the L/L interface. This technique was mainly used with the purpose of ensuring that the focus was made at the interface, therefore, we did not went deeper in the understanding of the reasons for the darker patches. Subsequently, videos of Brownian motion of the latex microbeads were obtained employing phase contrast microscopy. Fig. 4B shows one representative image of the latex microbeads on DSPG film at the L/L interface ( $\pi = 9 \text{ mNm}^{-1}$ ). This image is a frame of a whole video recording the bead's Brownian displacements. Typical trajectories are shown in Fig. 4B (see the inset with an expanded image of the

movement for one of the beads). Only 2-D movements were taken into account for calculating the diffusion coefficients (typical movies can be found as supplementary material). In the case of the other phospholipids, the images of the microbeads obtained by contrast microscopy are very similar, but different rates of Brownian motion were observed.

Supplementary video related to this article can be found at <https://doi.org/10.1016/j.electacta.2018.05.118>.

The determination of the diffusion coefficients of microbeads at different lipid concentrations at the L/L interface was carried out, as described in section 2.3. It's important to remark that the D values informed were obtained from independent experiments and are the mean results of 40 individual pair of trajectories analyzed. Fig. 5 shows the D values obtained; for the movements of microbeads at a DSPG monolayer. As can be observed, higher lipid concentration at the interface leads to slower Brownian motion, and thus to smaller D values.

Diffusion coefficients of microbeads were also determined in films of DMPC and DSPC adsorbed at the liquid/liquid interface, the results are summarized in Fig. 6, where D values obtained for air/water interfaces are also included for comparison. As can be seen, significant differences in D values between air/water and liquid/liquid interfaces were obtained, with higher values for the latest, indicating a more fluid lipid film at this interface compared to the air/water one. On the other hand, at the L/L interface, the D values depend on the nature of the phospholipid, and higher D values are obtained as the mean molecular area of the monolayer decreases:  $D_{\text{DSPG}} < D_{\text{DSPC}} < D_{\text{DMPC}}$ . In the A/L interface, the D values of DSPG and DSPC are slightly different and very low due to the high viscosity of the monolayer while D value for DMPC is significantly higher than the first ones.

The above results were obtained in the absence of polarization at L/L interface, and are the expected considering that a decrease in the film stiffness usually correlates with a decrease in the solid character of the film [27]. The relevance of this work is based on the possibility of measuring both, surface pressure ( $\pi$ ) and D, under simultaneous polarization of the interface. In these experiments, DSPG film was first formed at the L/L interface at a  $\pi$  value equal to

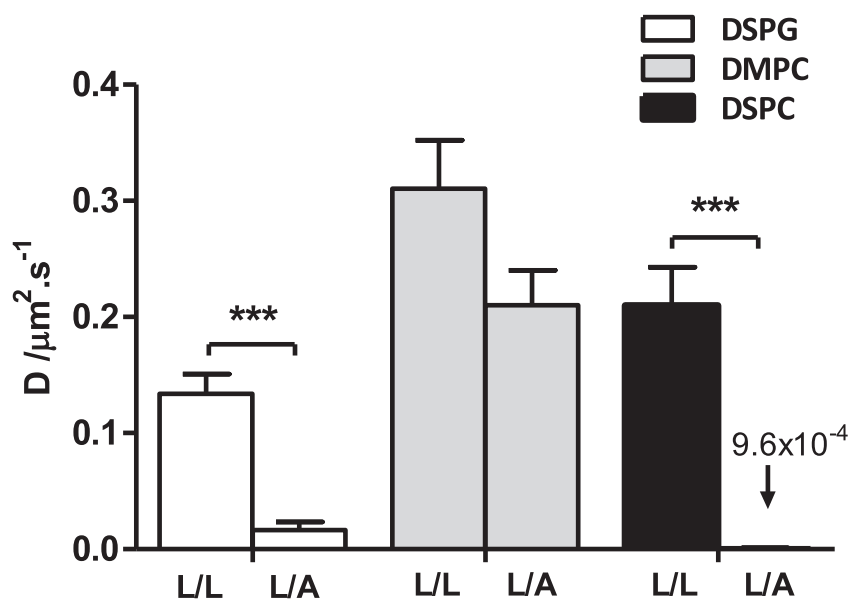


**Fig. 6.** Diffusion coefficients of latex beads at different monolayers: DSPG (white), DMPC (gray) and DSPC (black) adsorbed at L/L or A/L interfaces. Data are represented as mean  $D \pm SD$  of 40 individual pair of trajectories analyzed. (\*\*\*) indicates  $p < 0.001$  for the statistical difference between L/L vs L/A interfaces by Student's t-test.  $\pi = 9 \text{ mNm}^{-1}$  at L/L,  $20 \text{ mNm}^{-1}$  at L/A interface.

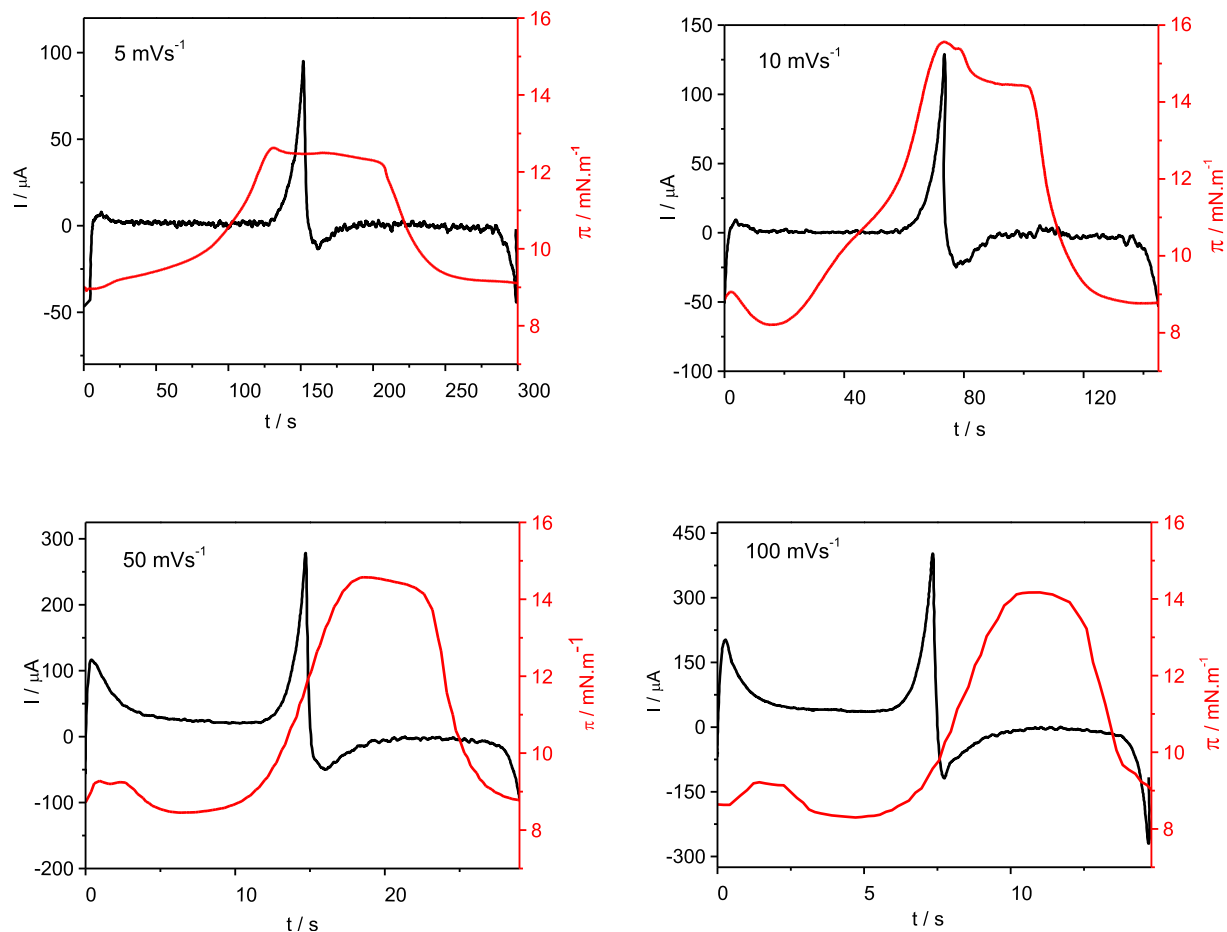


**Fig. 7.** Variation of  $\pi$  (red curve) and  $I$  (black curve) with time, during a cyclic voltammogram for a DSPG monolayer adsorbed at the liquid/liquid interface at different  $v$ . (Same figure represented as  $\pi$  and  $I$  vs  $E$  is shown in [Supporting Information](#)). (For interpretation of the references to colour in this figure legend, the reader is referred to the Web version of this article.)

$9 \text{ mN m}^{-1}$ , once a stable  $\pi$  value was obtained, the potential perturbation was carried on and the variation of  $\pi$  with time was recorded. Fig. 7 (A–D) shows the variation of  $\pi$ , and current,  $I$ , with time during a cyclic voltammetry experiment with films of DSPG at different scan rates,  $v$ . It can be observed that within the capacitive region,  $\pi$  values remain almost constant, while, in contrast, a sharp increase in  $\pi$  values is evident when a faradaic current is flowing. An important delay in  $\pi$  response, with respect to the voltammetric perturbation, is observed as  $v$  increases. This is very probably due to a delay in time response of the surface pressure sensor, since it was also observed in experiments carried out in the absence of the monolayer (not shown). It can also be noted that, at the end of the voltammogram,  $\pi$  values return to the initial values. It is worthwhile clarifying that the maximum changes in  $\pi$  values registered for a bare interface, in absence of the monolayer, during the voltammetric sweep, is only  $1 \text{ mN m}^{-1}$ , at all sweep rates studied (data not shown). It is worthwhile to remark at this point that the presence of Wilhelmy Pt plate within an electric field can act as a bipolar electrode producing an electrocatalytic current as reported by P. Peljo et al. [38] Nevertheless, when cyclic voltammetry experiments were carried out in the presence or the absence of the Wilhelmy plate at the interface, only a slight capacitive effect was observed. Additionally, potential steps, at  $E = 0.950$ ,  $0.450$  and  $0.200 \text{ V}$ , were also applied to the liquid/liquid interface during  $60 \text{ s}$ . As can be observed in the voltammogram shown in Fig. 8 A, faradic current takes place at  $E = 0.950$  and  $0.200 \text{ V}$ , while capacity current

predominates at  $E = 0.450 \text{ V}$ . As described before, once a stable  $\pi$  value was obtained, the potential step was applied and the variation of  $\pi$  with time was recorded (see Fig. 8 C). At  $E = 0.450 \text{ V}$ , the  $\pi$  value increases during the pulse (first  $60 \text{ s}$ ), and it decreases after the potential is turned off reaching an almost constant value of  $8 \text{ mN m}^{-1}$ , close to the initial one, indicating that the monolayer was not affected by this potential perturbation. In contrast, when the potential steps in the faradaic region were applied, a decrease in  $\pi$  values is observed during the perturbation, after which the initial conditions were not recovered. These results suggest that polarization at these extreme potential values, where ion transfer processes occur, produces a partial desorption of phospholipids molecules from the interface, producing an irreversible modification of the film.

Finally, we analyzed the effect of both kinds of interfacial polarization (cyclic voltammetry and potential steps) on the  $D$  values, observing the trajectories of the latex beads at the liquid/liquid interface modified with a DSPG monolayer, as described above. Fig. 9 shows the  $D$  values obtained for all experiments carried out, expressed as mean of 40 individual trajectories analyzed and the 95% confidence interval. Student's t-test was applied comparing the system with and without perturbation, in pairs. In all cases, there are difference significant with 95% of confidence. The  $p$  values obtained were:  $p = 0.03$  for CV experiments,  $p < 0.0001$  for P200,  $p = 0.0132$  for P450 and  $p = 0.0001$  for P950.

The most significant changes were obtained for potential steps

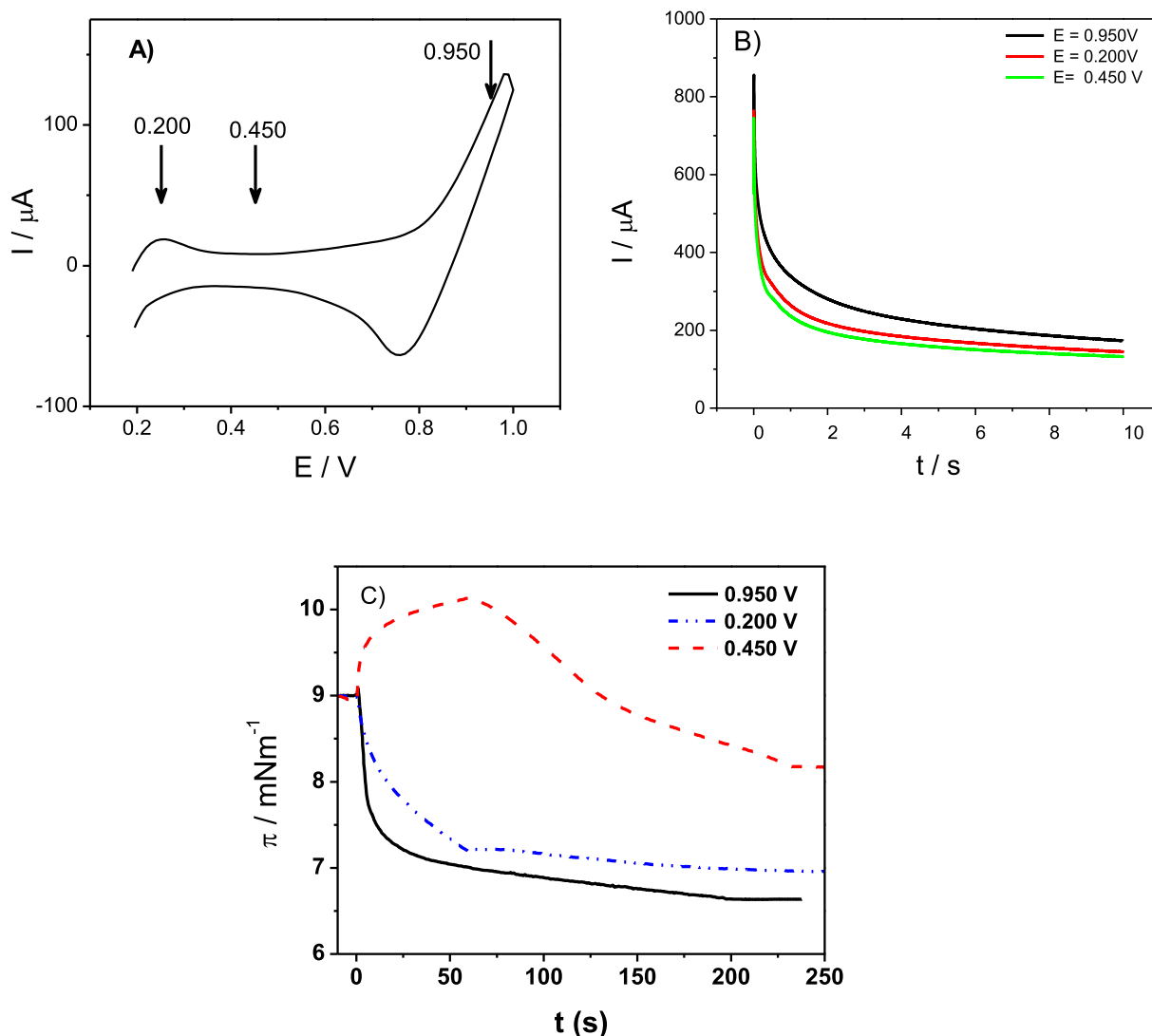


**Fig. 8.** A) Voltammogram recorded at  $v = 0.100 \text{ V}^{-1}$ . The arrows indicate the E values selected for potential steps experiments. B) Variation of  $I$  during the first 10 s of potential steps at  $E = 0.200, 0.450$  and  $0.95 \text{ V}$  vs  $\text{Ag}/\text{AgCl}$ . C)  $\pi$  variation with time during and after polarization at  $E = 0.950, 0.450$  and  $0.200 \text{ V}$  on  $L/L$  interface modified with an adsorbed DSPG monolayer. Polarization was applied during 60 s.

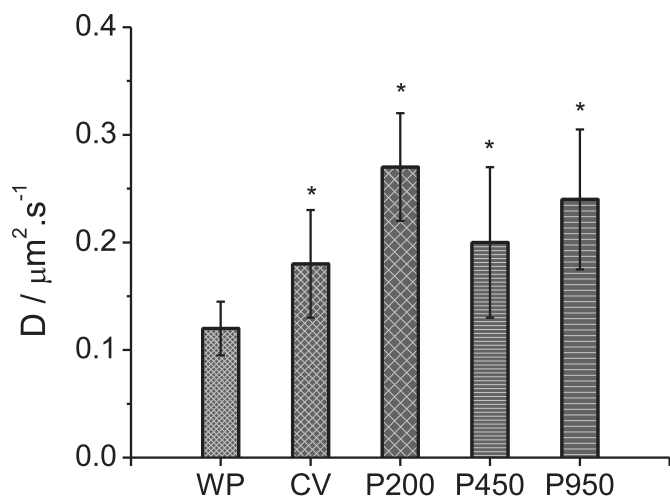


**Fig. 9.** Diffusion coefficient values obtained for microbeads on DSPG monolayers adsorbed at the  $L/L$  interface before and after potential perturbation,  $\pi_{\text{initial}} = 9 \text{ mNm}^{-1}$ : (WP) without polarization, (CV) after cyclic voltammetry perturbation and (P 0.200, P 0.450 and P 0.950 V) after different potential steps. Data are expressed as mean of 40 individual trajectories analyzed and bar are the 95% confidence interval. \* $p < 0.05$  indicates the statistical difference vs WP condition by Student's t-test.

at extreme values ( $E = 0.200$  and  $0.950 \text{ V}$ ). Under these conditions, we proposed that phospholipid molecules are removed from the interface, and thus, the initial rheological features of the monolayer are not restored. At  $E = 0.450 \text{ V}$ , a lower change in the rheological properties occurs, in concordance with the variation of  $\pi$  during this perturbation showed before. In the case of CV experiments, the change in  $D$  values is the lowest, pointing out that this kind of perturbation probably allows a lipids reorganization at the interface, while potential is changing, and loss of phospholipids molecules is not observed. This behavior is also in concordance with the variation of  $\pi$  values recorded during CV experiment (Fig. 8): pressure values restore to almost the initial values when the perturbation ends.

#### 4. Conclusions

We have demonstrated that the single-particle Brownian dynamics methodology, followed by optical microscopy, can be applied to liquid/liquid interfaces, in a similar way than in the case of air/water interfaces and it is a useful tool to evaluate the fluidity and solid character of phospholipid monolayers adsorbed at these interfaces. Moreover, the combination, for the first time, of this methodology with determinations of the interfacial surface

pressure and electrochemical techniques applied to liquid/liquid interfaces allowed as to determine the effect of polarization on the state of the monolayer with the advantage that the analysis can be made at any time, before, during and after the perturbation.

The combination of both techniques would appear to have great potential for the investigation of the rheological properties of a wide range of films composed by molecules of different nature, adsorbed at liquid/liquid interfaces.

## Acknowledgments

Financial support from FonCyT, CONICET and SECyT, UNC is gratefully acknowledged. A.V.J, N.W. and L.M.Y are members of the Research Career of CONICET. Andrea Juárez wishes to thank CONICET for the fellowships awarded. The authors greatly acknowledge the technical and imaging assistance of Dra. Cecilia Sampedro from the Centro de Microscopía Óptica y Confocal de Avanzada, CIQUIBIC-INIMEC-CIBICI, CONICET-Universidad Nacional de Córdoba, Córdoba, Argentina.

## Appendix A. Supplementary data

Supplementary data related to this article can be found at <https://doi.org/10.1016/j.electacta.2018.05.118>.

## References

- [1] L.M.A. Monzon, L.M. Yudi, Electrochemical study of flunitrazepam partitioning into zwitterionic phospholipid monolayers, *Electrochim. Acta* 51 (2006) 1932.
- [2] L.M.A. Monzon, L.M. Yudi, Flunitrazepam effect on distearoylphosphatidylglycerol, cholesterol and distearoylphosphatidylglycerol + cholesterol mixed monolayers structure at a DCE/water interface, *Electrochim. Acta* 51 (2006) 4573.
- [3] L.M.A. Monzon, L.M. Yudi, Cation adsorption at a distearoylphosphatidic acid layer adsorbed at a liquid/liquid interface, *Electrochim. Acta* 52 (2007) 6873.
- [4] M.V. Colqui Quiroga, L.M.A. Monzon, L.M. Yudi, Voltammetric study and surface pressure isotherms describing Flunitrazepam incorporation into a distearoylphosphatidic acid film adsorbed at air/water and water/1,2-dichloroethane interfaces, *Electrochim. Acta* 56 (2011) 7022.
- [5] M.V. Colqui Quiroga, L.M.A. Monzon, L.M. Yudi, Interaction of trifluoromazine with distearoylphosphatidylglycerol films studied by surface pressure isotherms and cyclic voltammetry at a 1,2-dichloroethane/water interface, *Electrochim. Acta* 55 (2010) 5840.
- [6] R.A. Walker, J.A. Gruetzmacher, G.L. Richmond, Phosphatidylcholine monolayer structure at a liquid-liquid interface, *J. Am. Chem. Soc.* 120 (1998) 6991.
- [7] R. Roozeman, P. Liljeroth, C. Johans, D.E. Williams, K. Kontturi, Dynamic interfacial tension at electrified liquid/liquid interfaces, *Langmuir* 18 (2002) 8318.
- [8] H. Jänchenová, K. Štulík, V. Mareček, Adsorption and ion-pairing interactions of phospholipids in the system of two immiscible electrolyte solutions. Part II: the formation and behavior of a lecithin layer at the water/1,2-dichloroethane interface in the presence of multivalent anions in the aqueous phase, *J. Electroanal. Chem.* 604 (2007) 109.
- [9] T. Kakiuchi, M. Kotani, J. Noguchi, M. Nakanishi, M. Senda, Phase transition and ion permeability of phosphatidylcholine monolayers at the polarized oil/water interface, *J. Colloid Interface Sci.* 149 (1992) 279.
- [10] M.C. Martins, C.M. Pereira, H.A. Santos, R. Dabirian, F. Silva, V. Garcia-Morales, J.A. Manzanares, Analysis of adsorption of phospholipids at the 1,2-dichloroethane/water interface by electrochemical impedance spectroscopy: a study of the effect of the saturated alkyl chain, *J. Electroanal. Chem.* 599 (2007) 367.
- [11] M.V. Colqui Quiroga, L.M.A. Monzon, L.M. Yudi, Interaction of trifluoromazine with distearoylphosphatidylglycerol films studied by surface pressure isotherms and cyclic voltammetry at a 1,2-dichloroethane/water interface, *Electrochim. Acta* 55 (2010) 5840.
- [12] D. Grandell, L. Murtomäki, G. Sundholm, Ion transfer across a phospholipid monolayer adsorbed at the water|1,2-dichloroethane interface under surface pressure control, *J. Electroanal. Chem.* 469 (1999) 72.
- [13] P. Liljeroth, A. Mälikä, V.J. Cunnane, A.K. Kontturi, K. Kontturi, Langmuir–Blodgett monolayers at a Liquid–Liquid interface, *Langmuir* 16 (2000) 6667.
- [14] A. Mälikä, P. Liljeroth, A.K. Kontturi, K. Kontturi, Electrochemistry at lipid monolayer-modified Liquid–Liquid interfaces as an improvement to drug partitioning studies, *J. Phys. Chem. B* 105 (2001) 10884.
- [15] A. Malkia, P. Liljeroth, K. Kontturi, Membrane activity of ionisable drugs – a task for liquid–liquid electrochemistry? *Electrochem. Commun.* 5 (2003) 473.
- [16] H. Jänchenová, A. Lhotsky, V. Mareček, Langmuir–Blodgett monolayers at an aqueous pendant drop, *Electrochim. Acta* 44 (1998) 161.
- [17] L.M.A. Monzon, L.M. Yudi, Flunitrazepam effect on distearoylphosphatidylglycerol, cholesterol and distearoylphosphatidylglycerol + cholesterol mixed monolayers structure at a DCE/water interface, *Electrochim. Acta* 51 (2006) 4573.
- [18] L.M. Yudi, E. Santos, A.M. Baruzzi, V.M. Solís, Erythromycin transfer across the water/1,2-dichloroethane interface modified by a phospholipid monolayer, *J. Electroanal. Chem.* 379 (1994) 151.
- [19] S.G. Chesniuk, S.A. Dassie, L.M. Yudi, A.M. Baruzzi, Valinomycin adsorption at the water/1,2-dichloroethane interface. Effect on cation-transfer processes, *Langmuir* 14 (1998) 5226.
- [20] C.I. Cámara, M.V. Colqui Quiroga, N. Wilke, A. Jimenez-Kairuz, L.M. Yudi, Effect of chitosan on distearoylphosphatidylglycerol films at air/water and liquid/liquid interfaces, *Electrochim. Acta* 94 (2013) 124.
- [21] C.I. Cámara, J.S. Riva, A.V. Juárez, L.M. Yudi, Interaction of chitosan and self-assembled distearoylphosphatidic acid molecules at liquid/liquid and air/water interfaces. Effect of temperature, *J. Phys. Org. Chem.* 29 (2016) 672.
- [22] T. Kakiuchi, M. Nakanishi, M. Senda, The electrocapillary curves of the phosphatidylcholine monolayer at the polarized oil–water interface. II. Double layer structure of dilauroylphosphatidylcholine, *Bull. Chem. Soc. Jpn.* 62 (1989) 403.
- [23] T. Kakiuchi, M. Kotani, J. Noguchi, M. Nakanishi, M. Senda, Phase transition and ion permeability of phosphatidylcholine monolayers at the polarized oil/water interface, *J. Colloid Interface Sci.* 149 (1992) 279.
- [24] V. Mareček, A. Lhotsky, H. Jänchenová, Mechanism of lecithin adsorption at a Liquid/Liquid interface, *J. Physiol. Biochem.* 107 (2003) 4573.
- [25] K. Maeda, Y. Yoshida, T. Goto, V. Mareček, Blocking effect of a phospholipid monolayer on ion transfer at a liquid/liquid interface and its electrochemical control, *J. Electroanal. Chem.* 567 (2004) 317.
- [26] N. Wilke, B. Maggio, The influence of domain crowding on the lateral diffusion of ceramide-enriched domains in a sphingomyelin monolayer, *J. Phys. Chem. B* 113 (2009) 12844.
- [27] N. Wilke, F. Vega Mercado, B. Maggio, Rheological properties of a two phase lipid monolayer at the air/water interface: effect of the composition of the mixture, *Langmuir* 26 (2010) 11050.
- [28] C.I. Cámara, N. Wilke, Interaction of dextran derivatives with lipid monolayers and the consequential modulation of the film properties, *Chem. Phys. Lipids* 204 (2017) 34.
- [29] M. Sickett, F. Rondelez, H.A. Stone, Single-particle Brownian dynamics for characterizing the rheology of fluid Langmuir monolayers, *Europhys. Lett.* 79 (2007), 66005p1.
- [30] D.A. Peñalva, N. Wilke, B. Maggio, M.I. Aveladoño, M.L. Fanani, Surface behavior of sphingomyelins with very long chain polyunsaturated fatty acids and effects of their conversion to ceramides, *Langmuir* 30 (2014) 4385.
- [31] Y.M. Zulueta Díaz, M. Mottola, R.V. Vico, N. Wilke, M.L. Fanani, The rheological properties of lipid monolayers modulate the incorporation of l-ascorbic acid alkyl esters, *Langmuir* 32 (2016) 587.
- [32] F. Vega Mercado, B. Maggio, N. Wilke, Modulation of the domain topography of biphasic monolayers of stearic acid and dimyristoyl phosphatidylcholine, *Chem. Phys. Lipids* 165 (2012) 232.
- [33] A. Mangiarotti, N. Wilke, Electrostatic interactions at the microscale modulate dynamics and distribution of lipids in bilayers, *Soft Matter* 13 (2017) 686.
- [34] B. Caruso, M. Villarreal, L. Reinaudi, N. Wilke, Inter-domain interactions in charged lipid monolayers, *J. Phys. Chem. B* 118 (2014) 519.
- [35] D. Grandell, L. Murtomäki, Surface pressure control of phospholipid monolayers at the water/1,2-dichloroethane interface, *Langmuir* 14 (1998) 556.
- [36] S. Mafé, J.A. Manzanares, K. Kontturi, Phospholipid monolayers at water/oil interfaces: theoretical modelling of surface pressure–molecular area isotherms, *J. Electroanal. Chem.* 457 (1998) 155.
- [37] D.S. Alvares, N. Wilke, J. Ruggiero Neto, M.L. Fanani, The insertion of Polybia-MP1 peptide into phospholipid monolayers is regulated by its anionic nature and phase state, *Chem. Phys. Lipids* 207 (2017) 38.
- [38] P. Peljo, M.D. Scanlon, A.J. Olaya, L. Rivier, E. Smirnov, H.H. Girault, Redox electrocatalysis of floating nanoparticles: determining electrocatalytic properties without the influence of solid supports, *J. Phys. Chem. Lett.* 8 (2017) 3564.